

Supporting Information

Ethylene Dehydrogenation on Pt_{4,7,8} Clusters on Al₂O₃: Strong Cluster-Size Dependence Linked to Preferred Catalyst Morphologies

Eric T. Baxter,^{1,‡} Mai-Anh Ha,^{2,‡} Anastassia N. Alexandrova,^{2,3,*} Scott L. Anderson^{1,*}

¹*Department of Chemistry, University of Utah, Salt Lake City, UT 84112.* ²*Department of Chemistry and Biochemistry, University of California, Los Angeles, and* ³*California NanoSystems Institute, Los Angeles, CA 90095.*

[‡]Authors equally contributed to this work

*Corresponding Authors' emails: ana@chem.ucla.edu, anderson@chem.utah.edu

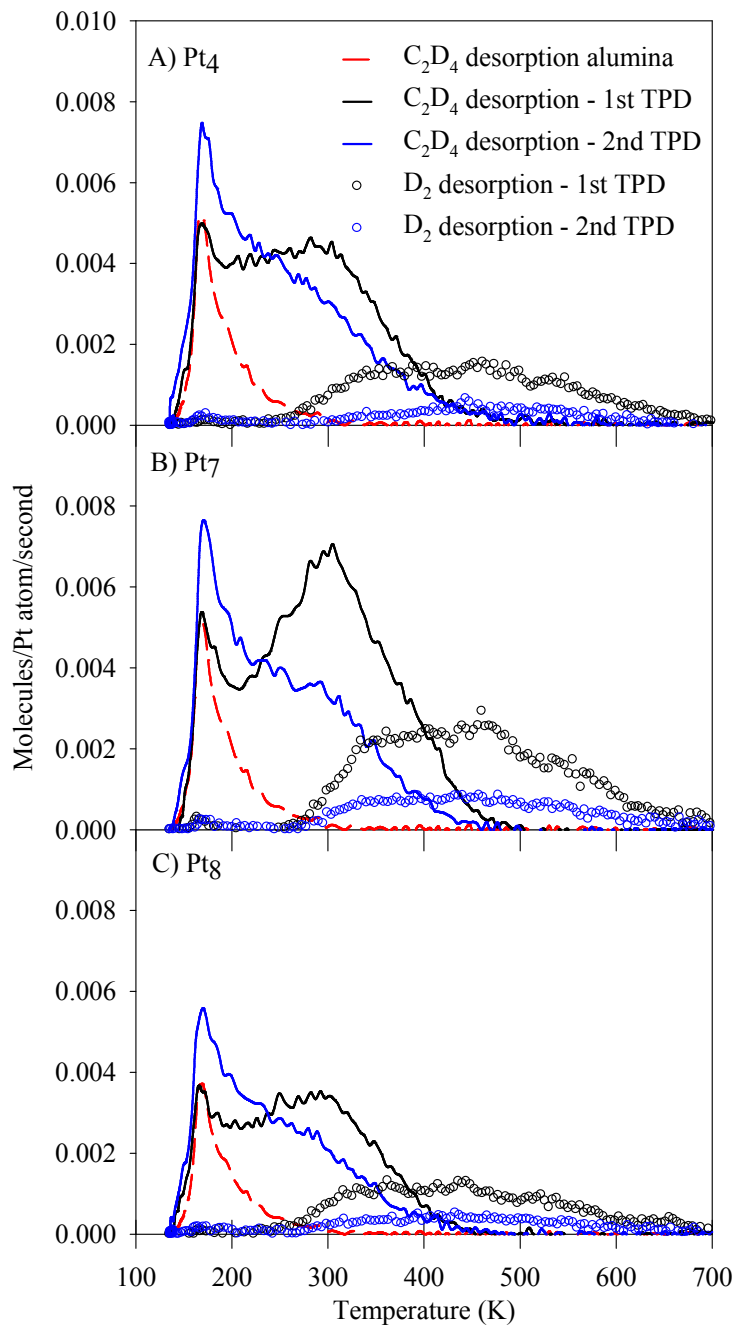


Figure S1. Intact C_2D_4 (solid) and D_2 (circles) desorbing from $\text{Pt}_n/\text{alumina/Ta}(110)$ ($n=4,7,8$) sample during two consecutive TPD measurements. Intact C_2D_4 (red dashed line) desorbing from a cluster free alumina/Ta(110) sample. All samples were exposed to 5 L of C_2D_4 at 150 K before starting the TPD measurement. The D_2 signal has not been corrected for the amount of D_2 produced from the fragmentation of C_2D_4 caused by electron impact ionization.

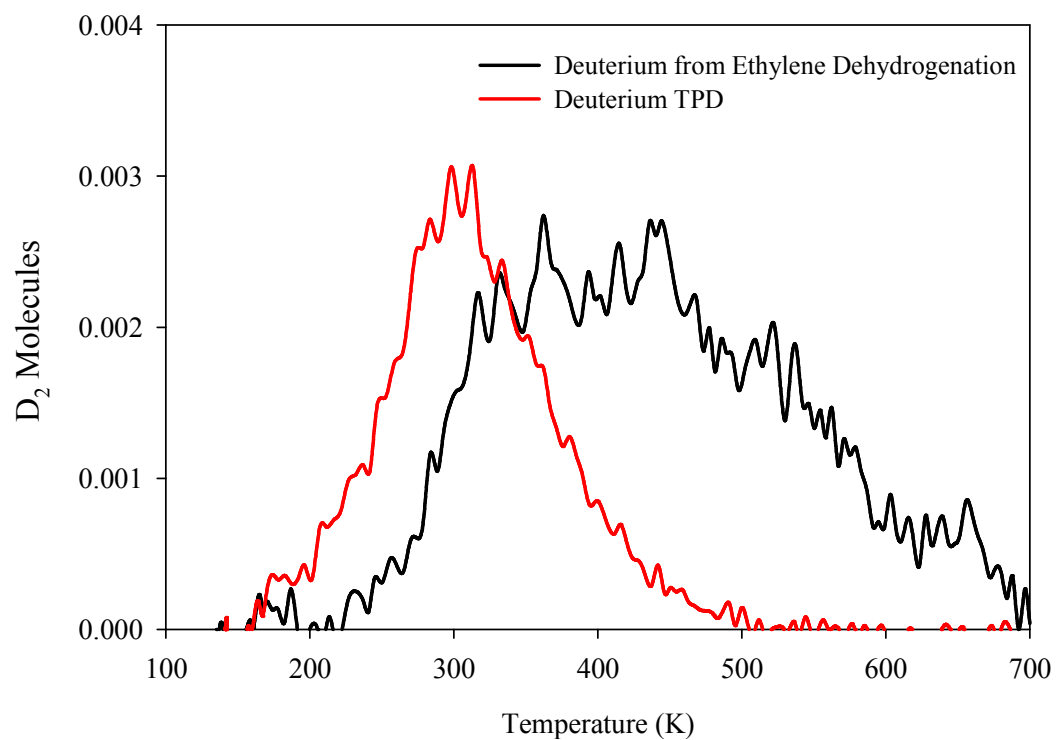


Figure S2. D_2 desorbing from $Pt_8/\text{alumina/Ta}(110)$ after exposing the sample to 5 L of D_2 at 150 K (red). D_2 produced by C_2D_4 dehydrogenation during a C_2D_4 TPD/R measurement (black).

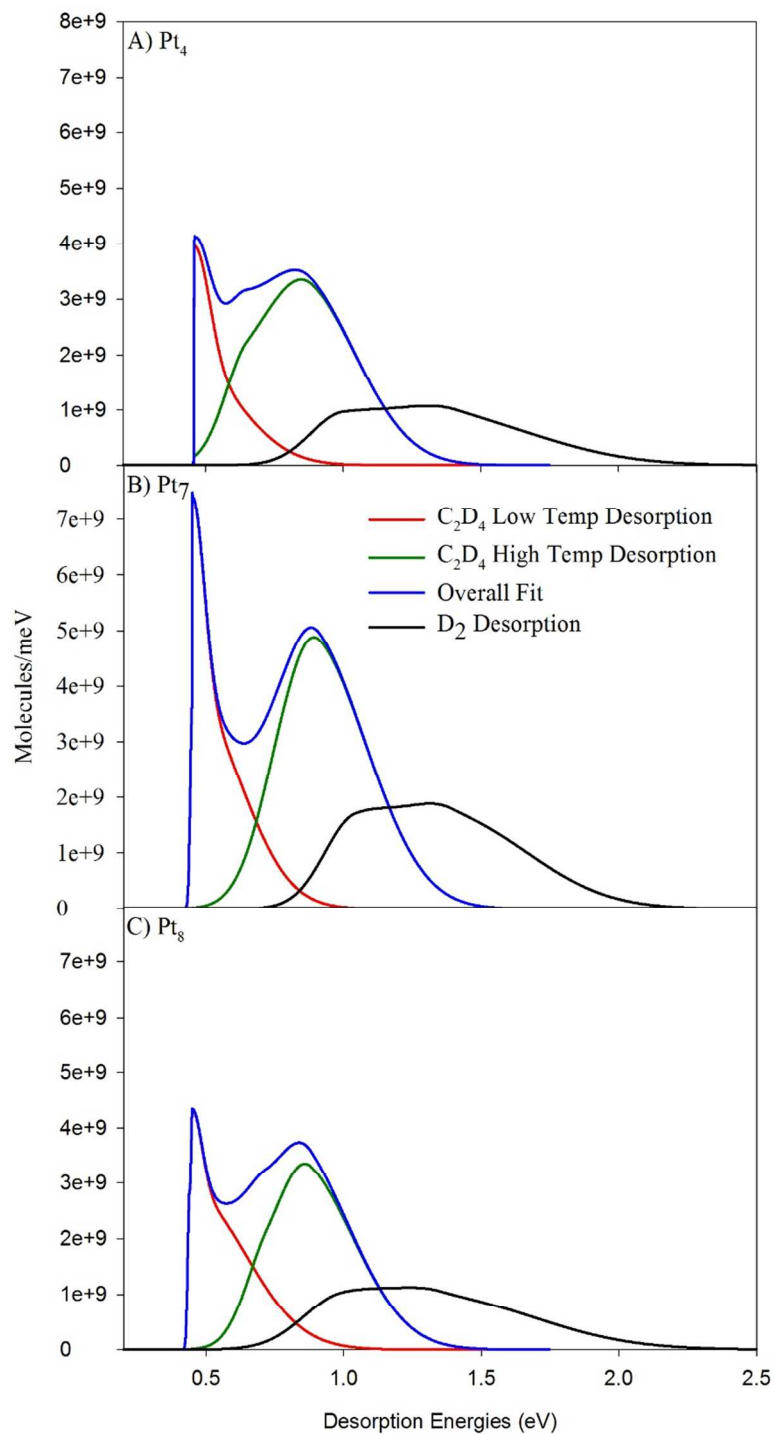


Figure S3. Energy of desorption fits for C_2D_4 and D_2 desorbing during the first C_2D_4 TPD/R experiments for Pt_4 , Pt_7 , and Pt_8

TPD fitting method and results:

A distribution of population in sites with different energies for desorption/dehydrogenation, $\theta(E)$, is assumed, and then the TPD/R spectra are fit using the first order rate equation:²⁰

$$I(t) \propto \frac{-d\theta}{dt} = (\theta(E) \cdot v) e^{\frac{-E}{kT(t)}},$$

where $I(t)$ is the desorption as a function of time, v is a prefactor and $T(t)$ is the temperature as a function of time. $\theta(E)$ is adjusted until the simulated $I(t)$ matches the experiment. Because size-selected cluster samples are time consuming to prepare, and irreversibly changed by a single TPD/TPR run, it is simply not practical to extract v from a series of coverage-dependent experiments on every cluster size. Therefore, the simulations were tested for v ranging from 10^{13} to 10^{15} s^{-1} , covering a range often found in TPD^{1,21}. The simulated desorption/dehydrogenation energies shift by only ~7% *per* order-of-magnitude variation in v , and in Figure S3 we present the $\theta(E)$ distributions obtained for $v = 10^{14} \text{ s}^{-1}$.

XPS results

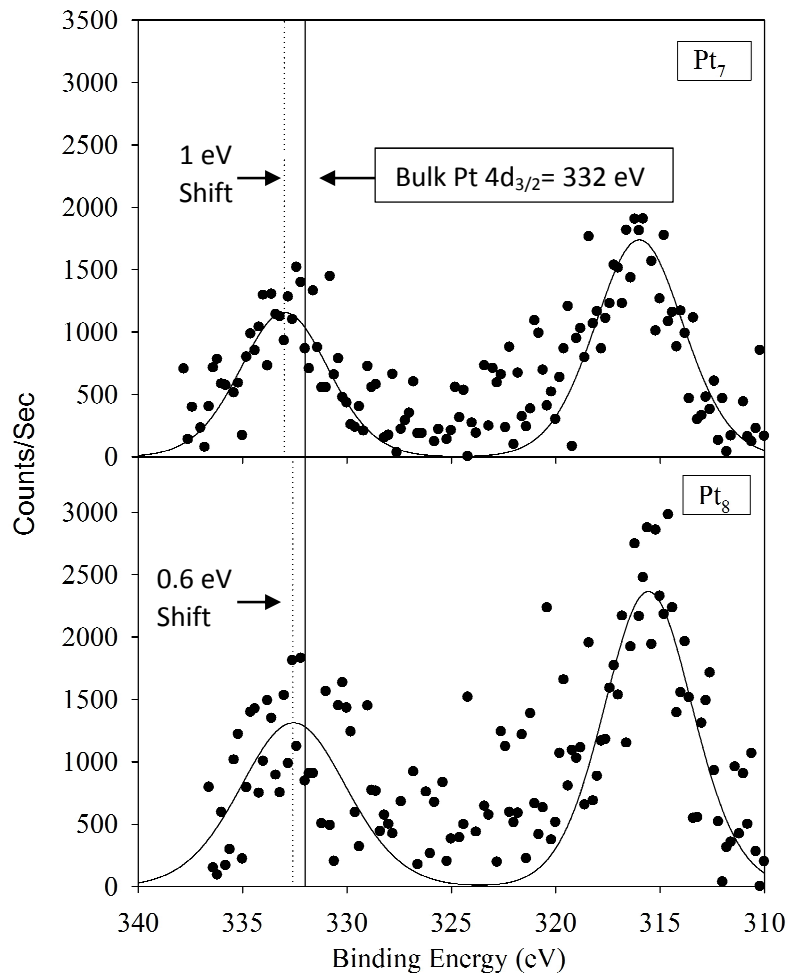


Figure S4. Pt 4d XPS for Pt₇ and Pt₈, as-deposited on alumina/Ta(110)

ISS extrapolation method

Figure S5 shows the normalized Pt ISS intensity as a function of He^+ exposure in a sequence of low He^+ flux ($0.1 \mu\text{A}$) ISS measurements. The increase in Pt signal during the initial measurements is evidence of a small coverage of adventitious adsorbates (CO and H_2O as determined by separate TPD measurements) that had adsorbed onto the clusters during the ~ 15 min cluster deposition time. The initial increase in Pt signal is a result of the adsorbates being sputtered off the cluster to expose the underlying Pt to He^+ scattering. The Pt signal eventually reaches a maximum and begins to decrease due to Pt sputtering. To determine the as-deposited value the Pt intensity is extrapolated back to the limit of zero He^+ exposure and zero adsorbate coverage as shown by the fit in Figure S5.

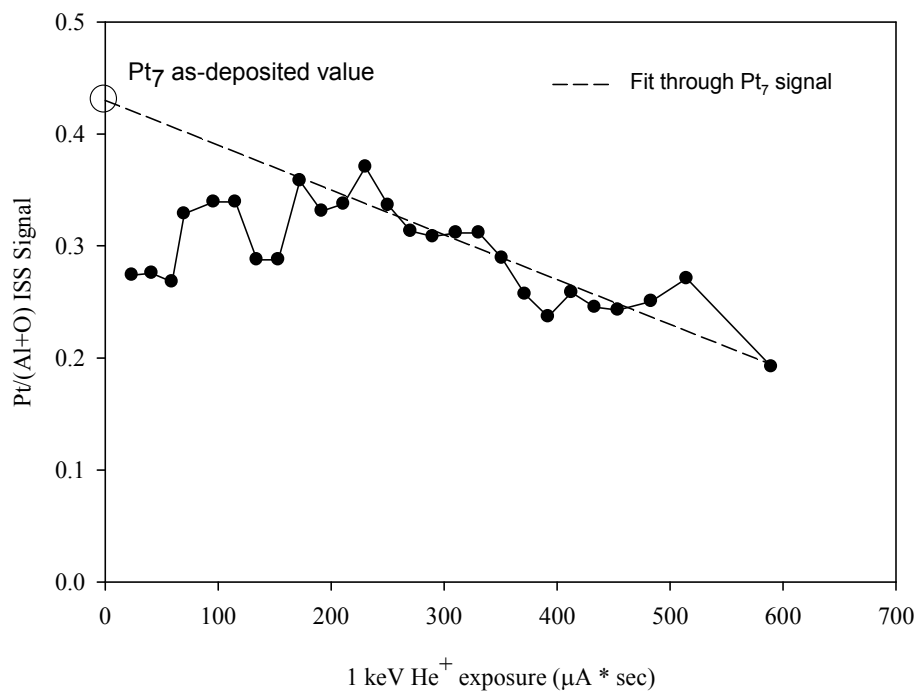


Figure S5. Normalized Pt intensity for Pt₇ as a function of He^+ exposure during a sequence of low He^+ flux ($0.1 \mu\text{A}$) ISS scans. The as-deposited value of the Pt intensity can be determined by extrapolating back to the limit of zero exposure and adsorbate coverage

Pt₄CO TD-ISS

Figure S6 shows the results from a ¹³C¹⁶O TPD and a TD-ISS experiment performed in our group by F. Sloan Roberts and Matthew Kane on the Pt₄/alumina/Re(0001) system. The ¹³C¹⁶O TPD (blue) measurement was collected by exposing a freshly prepared Pt₄/alumina/Re(0001) sample with 10 L of ¹³C¹⁶O at a 180 K. The sample was allowed to cool to 140 K before heating the sample at a rate of 3 K/sec while detecting the amount of ¹³C¹⁶O desorbing from the surface.

The TD-ISS measurements were collected by exposing a separately prepared Pt₄/alumina/Re(0001) sample to 10 L of ¹³C¹⁶O at 180 K and collecting an ISS spectrum with a single low He⁺ flux (0.1μA) scan. The succeeding points in the TD-ISS curve were collected by heating the sample in 50 K increments and measuring the ISS spectrum at the indicated temperatures. The loss of Pt signal due to sputtering, the recovery of Pt signal due to removal of ¹³C¹⁶O, and the as-deposited Pt signal are represented by sloping dashed lines and were determined on separately prepared samples using the same procedure that was used for Figure 2.

From the TPD results, heating the sample to 350 K desorbs ~35 % of the total ¹³C¹⁶O coverage but results in an insignificant recovery in the Pt ISS signal. As the sample is heated from 350 to 650 K there is a sharp recovery of the Pt ISS signal as the remaining ¹³C¹⁶O coverage desorbs. These results suggest that the weakly bound ¹³C¹⁶O that is desorbed at temperatures < 350 K is bound in sites that are inefficient at blocking or shadowing the He⁺ from scattering off the Pt, such as around the periphery of the cluster. On the other hand, the ¹³C¹⁶O desorbed at temperatures above 350 K leads to a strong recovery of the Pt ISS signal suggesting it desorbs from sites that efficiently attenuate the signal, such as on top sites.

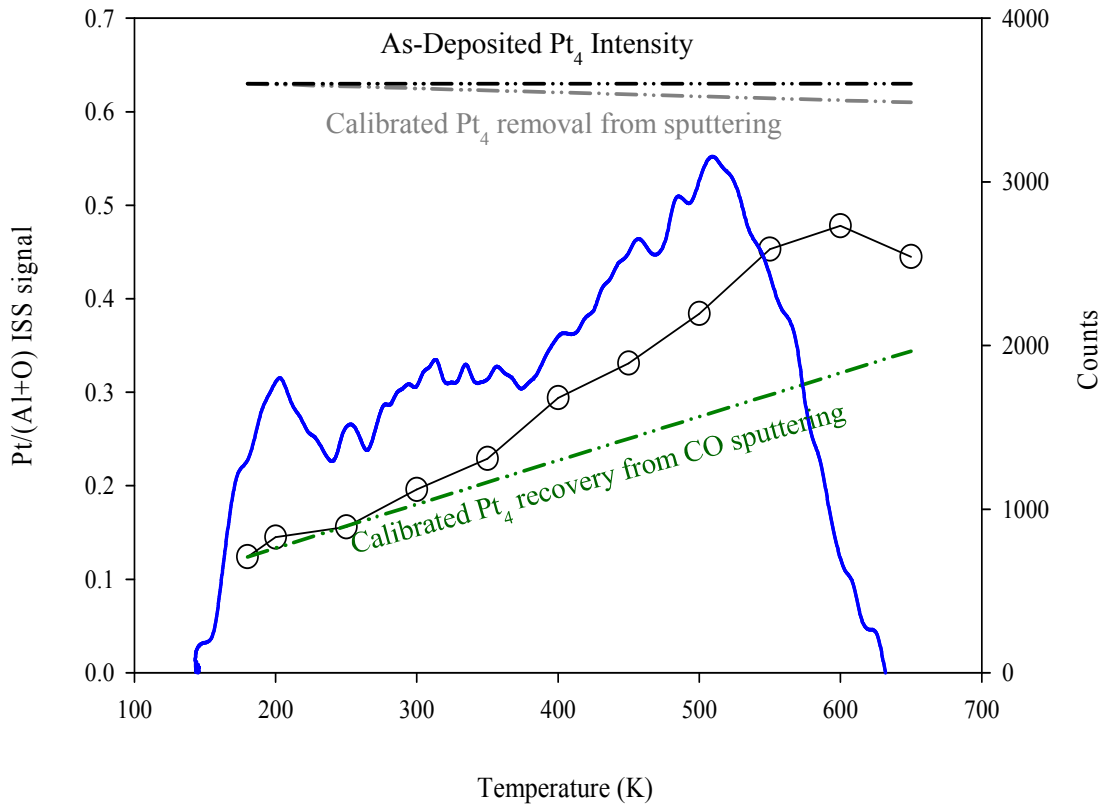


Figure S6. $\text{Pt}/(\text{Al}+\text{O})$ ISS signal as function of temperature (circles) after exposing the sample with 10 L of $^{13}\text{C}^{16}\text{O}$ at 180 K. CO desorbing from a separately prepared $\text{Pt}_4/\text{alumina}/\text{Re}(0001)$ sample exposed to 10 L of $^{13}\text{C}^{16}\text{O}$ at 180 K during the first TPD measurement (blue). Both samples contained a 0.1 ML of deposited Pt_4 clusters.

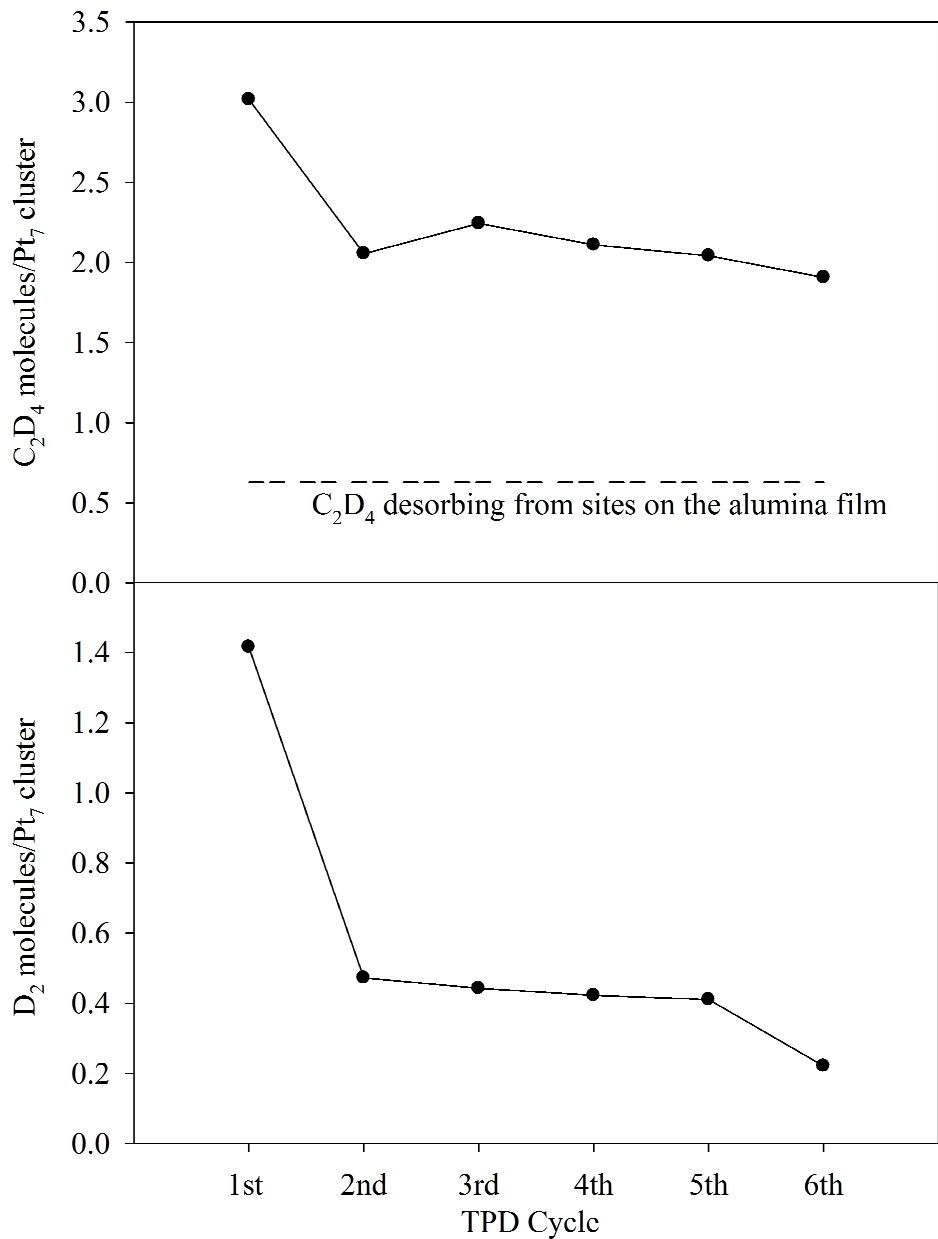


Figure S7. Integrated amounts of C_2D_4 (top) and D_2 (bottom) desorbing, *per* deposited Pt_7 cluster, during a sequence of 6 TPD/R runs under the conditions used in Fig. 2. The dashed horizontal line gives an estimate for the C_2D_4 desorbing from alumina sites, taken from the integrated desorption measured for cluster-free alumina.

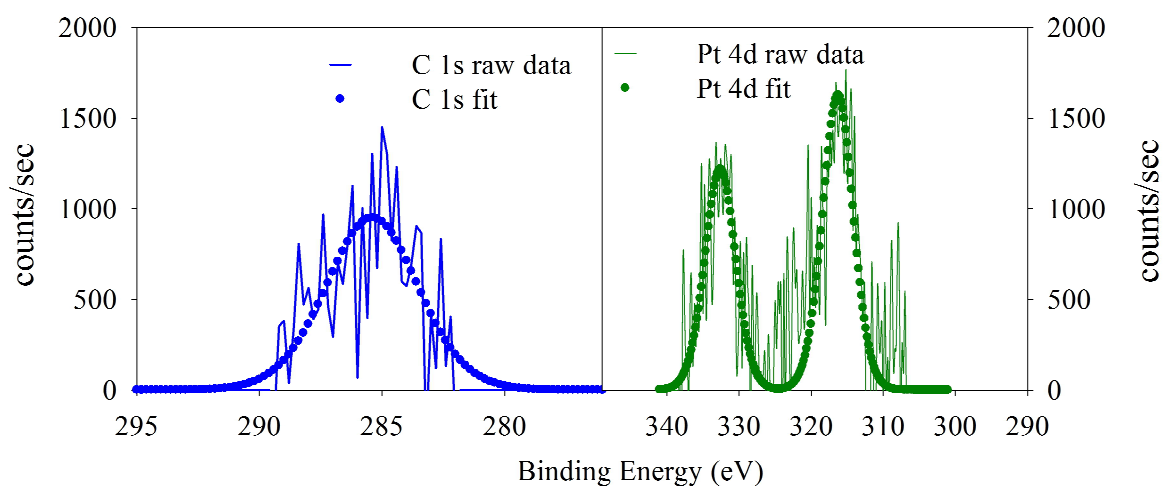


Figure S8. C 1s and Pt 4d peaks measured by XPS after 6 consecutive TPD cycles on a Pt₇/alumina sample. The presence of carbon suggest that dehydrogenation of ethylene leads to the deposition of carbon onto the model catalyst

Theoretical Methods - details

The relevant equations regarding formation (E_{form}), adsorption (E_{ads}), and sintering energies (E_s) are described in the following. E_{form} is VASP's DFT energy of the gas phase cluster with the component, atomic energies already subtracted. The atomic energies arise from the calculated energies of the elements from which the pseudopotential was generated.

$$E_{ads}[\text{Pt}_n] = E[\text{Surf+Pt}_n] - E[\text{Surf}] - E_{gas,min}[\text{Pt}_n]$$

where $E[\text{Surf+Pt}_n]$ is the total DFT energy of the supported cluster system, $E[\text{Surf}]$ is the total energy of the bare support, and $E_{gas,min}[\text{Pt}_n]$ is the global minimum of the gas-phase cluster.

An analogous equation to E_{ads} for reagent species ($reag$) such as ethylene and C (a single carbon atom is used as a first-order approximation to coking) is detailed below:

$$E_{reag} = E[\text{Surf+Pt}_n+reag] - E[\text{Surf+Pt}_n] - E_{reag}$$

where $E[\text{Surf+Pt}_n+reag]$ is the total DFT energy of the supported cluster system with the reagent species and E_{reag} is the total energy of the gas-phase cluster. In coverage calculations of ethylene, E_{reag} will encompass the $n \times E_{ethyl}$, where E_{ethyl} is the energy of ethylene in the gas-phase.

Statistical analysis is performed through use of the Boltzmann probability for i -th configuration (P_i) by taking the Boltzmann distribution of each minimum ($e^{-E_i/k_B T}$) divided by the sum of the distributions of all relevant low energy minima:

$$P_i = \frac{e^{-E_i/k_B T}}{\sum e^{-E_i/k_B T}}$$

where E_i is the i -th configuration energy of a gas phase cluster (i.e. E_{form} as defined above), adsorbed cluster ($E[\text{Surf+Pt}_m B_n]$) or adsorbed cluster with a reagent ($E[\text{Surf+Pt}_n+reag]$), k_B is the Boltzmann constant, and T is the temperature.

The entropic contribution of relevant minima may also be found by considering the fundamental thermodynamic relation of the Helmholtz free energy ($F = U - TS$). Specifically, the Gibbs' entropy equation (S_G) allows us to analyze the effect of discrete states with their respective Boltzmann probabilities on the ensemble of particular cluster types:

$$S_G = -k_B \sum_i P_i \ln(P_i)$$

where the P_i are the Boltzmann weights and k_B is the Boltzmann constant. In this way, we may analyze the entropic contribution at a catalytically relevant temperature (TS_G).

In the gas phase, the septamer and octamer contain many isomers whose energies are within 0.2-0.3 eV of the most stable geometry (Figure S9).^{1,2} The gas phase isomers present a mixture of 2D and 3D geometries. Adsorbed structures were formed from the deposition of the lowest 5-6 gas phase structures, with a thorough sampling of cluster faces to possible binding sites. The complexity of the corrugated alumina surface leads to a combination of Pt-Al and Pt-O coordination so that single-layer gas phase isomers crinkle in order to maximize wetting of the surface (observed in Pt₇, Isomer II, Main text Fig. 1). As the surface is Al-terminated, Pt coordinating to electropositive Al gains a negative charge. Likewise, Pt-O coordination yields positively charged Pt so that a single cluster features a range of electronic depletion or augmentation from one atom to the next. These atomic charges (Δq) are visualized in the main text's Fig. 1. The charge separation between atoms yields an electrostatic potential that further stabilizes clusters and attenuates their site reactivity.

There is an apparent switch in dimensionality between Pt₇ to Pt₈, where Pt₇ on average features more open geometries that wet the corrugated support. The adsorbed Pt₇ clusters feature a prismatic geometry ($\Sigma P_{700K} = 66.67\%$, Isomers I and IV) and a single-layer geometry ($\Sigma P_{700K} = 33.33\%$, Isomers II, III, and V). This mix of structures offers a complex and rich set of binding sites for adsorbates. In contrast, all of the isomers of Pt₈ are prismatic. In prismatic structures, some of the Pt atoms are buried inside the cluster, becoming unavailable as binding sites. These results are in agreement with the experimental findings that suggest that Pt₇ provides more binding sites for ethylene as compared to Pt₈. Additionally, there is a greater uniformity in the nature of the exposed binding sites, as can be judged by their partial charges. The septamer optimizes the cluster-support interactions with a relatively high charge transfer ($\Delta Q > -1.20$ e) in the global minimum, and, unsurprisingly, features the most favorable adsorption. The added negative charge does not distribute uniformly over the cluster; instead, there is a polarization of Pt atoms in Pt₇. Pt₈ preserves the charge transfer behavior of Pt₇, but adsorption to the support is weaker: of the global minimum of Pt₈, Pt_{8,glob}, it is 0.2 eV weaker than that of Pt_{7,glob}. The Pt atoms within Pt_{8,glob} are charged more uniformly (details in Table S4).

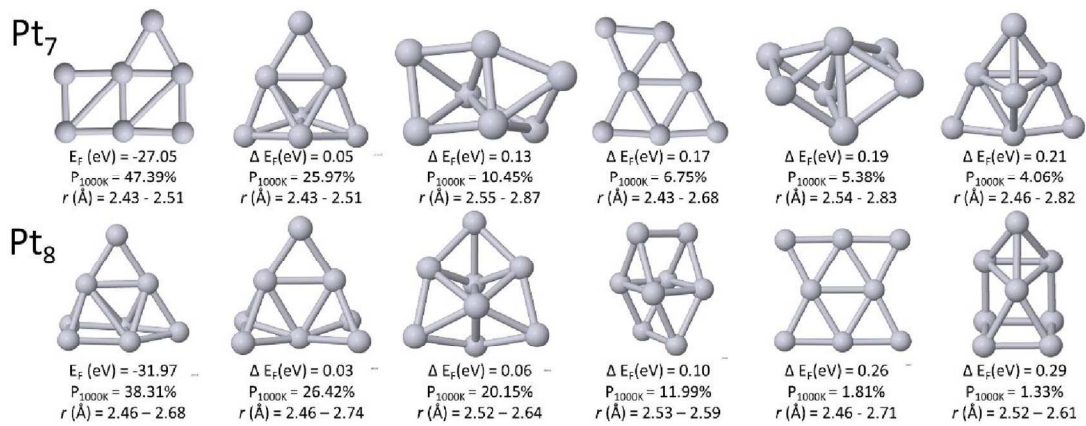


Figure S9. Gas phase isomers of Pt₇, Pt₈ at catalytically relevant temperature of 1000K

Table S1. Formation energies of global minima of Pt₇, Pt₈

	Pt ₇	Pt ₈
E _{form} (eV)	-27.05	-31.97
E _{form/atom} (eV)	-3.86	-4.00

Table S2. Gas phase isomers

Cluster	Isomer	Δ E _{form} (eV)	P _{450 K}	P _{1000 K}
Pt ₇	I	0.00	75.60%	47.39%
	II	0.05	19.85%	25.97%
	III	0.13	2.63%	10.45%
	IV	0.17	0.99%	6.75%
	V	0.19	0.60%	5.38%
	VI	0.21	0.32%	4.06%
Pt ₈	I	0.00	56.98%	38.31%
	II	0.03	24.95%	26.42%
	III	0.06	13.66%	20.15%
	IV	0.10	4.31%	11.99%
	V	0.26	0.06%	1.81%
	VI	0.29	0.03%	1.33%

Table S3. Gas phase isomers under def2/TZVPP basis with pure and hybrid functionals calculated in TURBOMOLE V6.6

Cluster	Isomer	Δ E _{form} (eV), Multiplicity				
		VASP	TM/PBE	TM/PBE0	TM/TPSS	TM/TPSSh
Pt ₇	I	0.00	0.00, 5	0.86, 5	0.34, 5	0.65, 5
	II	0.05	0.15, 5*	0.36, 5, I	0.18, 5	0.32, 5, I
	III	0.13	0.01, 5	0.00, 5	0.00, 5	0.00, 5
	IV	0.17	0.20, 5, I	0.72, 5	0.40, 3*	0.71, 3
	V	0.19	0.05, 5	0.31, 5, I	0.10, 5	0.15, 5
	VI	0.21	0.20, 5*	0.40, 5, I	0.26, 5*	0.16, 5

* geometries had difficulty converging, I = geometries with an imaginary frequency

Table S4. Adsorbed isomers of Pt₇, Pt₈ with Boltzmann populations (P) at experimentally relevant temperatures of 450 and 1000 K and charge transfer (ΔQ) from the support

Cluster	Isomer	ΔE_{ads} (eV)	P _{450 K}	P _{700 K}	ΔQ (e)
Pt ₇	I	0.00	75.27%	65.89%	-1.22
	II	0.04	24.49%	32.02%	-1.44
	III	0.24	0.16%	1.26%	-1.33
	IV	0.27	0.07%	0.77%	-1.25
	V	0.43	<0.01%	0.05%	-1.23
	$\Sigma P_T E_{\text{ads}}$ (eV)	-5.08	-5.07		
Pt ₈	TS _G (eV)	0.010	0.019		
	I	0.00	97.65%	87.73%	-1.24
	II	0.17	1.14%	5.03%	-1.07
	III	0.19	0.74%	3.82%	-0.94
	IV	0.21	0.41%	2.61%	-1.08
	V	0.30	0.04%	0.57%	-1.22
	VI	0.39	<0.01%	0.14%	-1.08
	VII	0.41	<0.01%	0.10%	-0.80
	$\Sigma P_T E_{\text{ads}}$ (eV)	-4.89	-4.87		
	TS _G (eV)	0.002	0.009		

Table S5. Local minima of adsorbed ethylene on Pt₇ (Isomer I and II)

Ads.	Config.	$\Delta E_{\text{ethylene}}$ (eV)	P _{450 K}	P _{700 K}	$\Delta Q_{\text{ethylene}}$ (e)	Hybrid.	C-C Bond Lengths (Å)	Bond Angles (°)
Pt ₇ , Isomer I	i	0.00	86.93%	72.48%	0.00	sp2	1.41	115.4–120.5
	ii	0.10	7.35%	14.81%	-0.07	sp3	1.49	100.6–114.9
	iii	0.11	5.72%	12.59%	0.00	sp2	1.40	116.0–120.5
	iv	0.38	<0.01%	0.13%	-0.16	sp3	1.49	99.7–115.4
	v	0.79	<0.01%	<0.01%	-0.10	sp3	1.50	97.5–114.9
	vi	0.87	<0.01%	<0.01%	-0.02	sp3	1.51	100.6–113.9
Pt ₇ , Isomer II	i	0.00	99.64%	96.30%	0.01	sp2	1.42	115.0–120.5
	ii	0.24	0.22%	1.90%	-0.01	sp2	1.41	114.6–121.0
	iii	0.26	0.12%	1.26%	-0.05	sp3	1.49	97.5–115.9
	iv	0.34	0.02%	0.36%	-0.03	sp2	1.42	114.8–120.4
	v	0.39	<0.01%	0.15%	-0.03	sp2	1.42	115.3–120.4
	vi	0.49	<0.01%	0.03%	-0.05	sp3	1.50	100.4–115.5

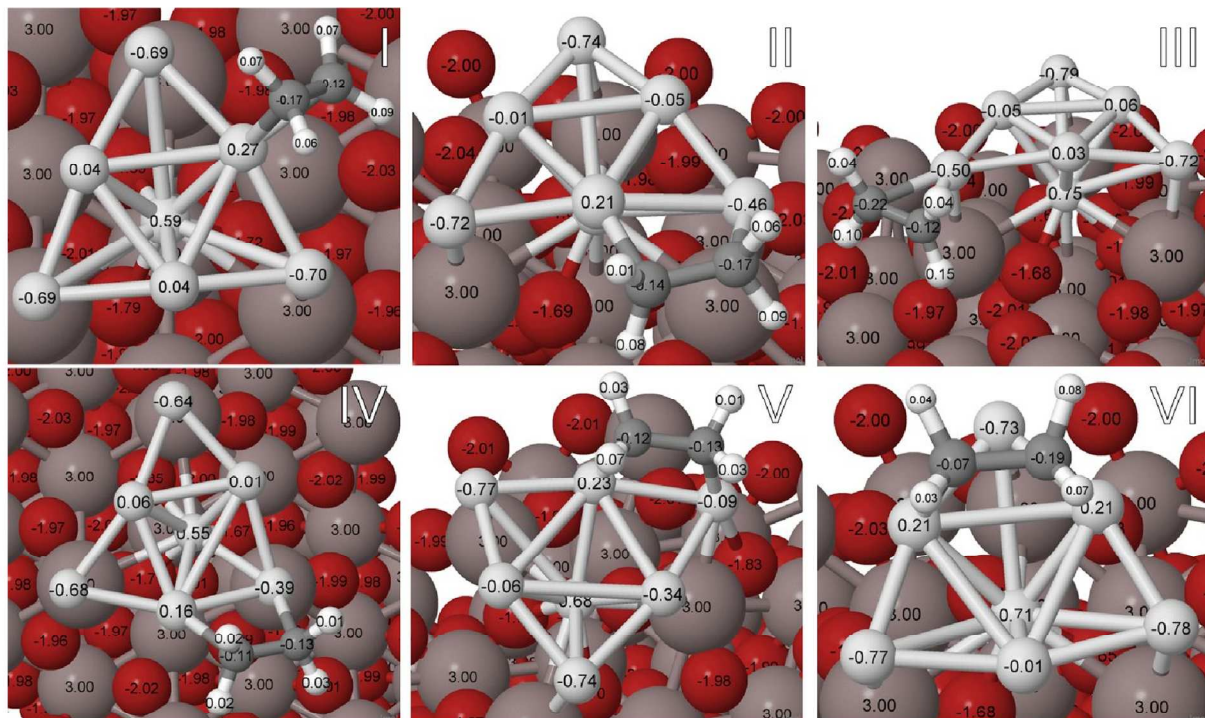


Figure S10. The lowest minima of ethylene adsorbed on $\text{Pt}_7\text{,glob}$, with calculated Bader charges.

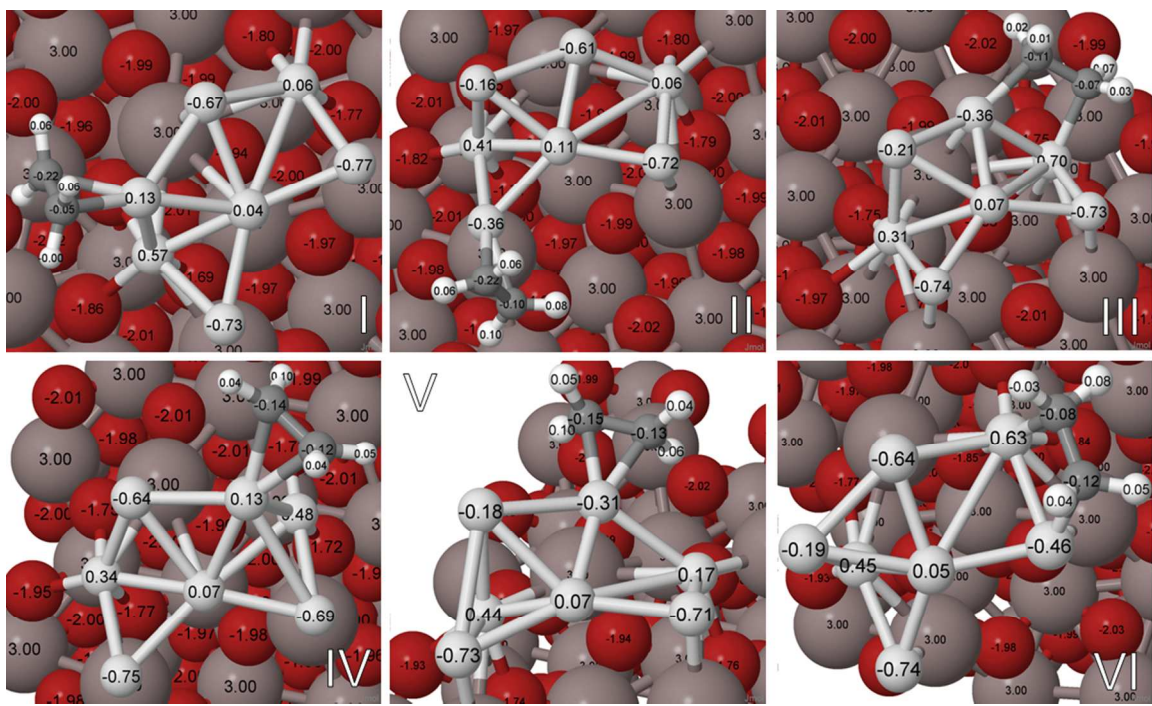


Figure S11. The lowest minima of ethylene adsorbed on the second lowest minimum of adsorbed Pt₇, with calculated Bader charges.

Table S6. Local minima configurations of a coverage of 2 ethylene on Pt₇,_{glob}

Configurations	P _{450 K}	P _{700 K}	ΔE	ΔQ _{Ethylene (e)}	Hybrid.
I	82.13%	67.60%	0.00	-0.02	sp2
II	15.45%	23.10%	0.06	-0.11	sp2, sp3
III	2.06%	6.32%	0.14	-0.08	sp2, sp3
IV	0.18%	1.32%	0.24	0.01	sp2
V	0.11%	0.96%	0.26	-0.02	sp2
VI	0.07%	0.70%	0.28	-0.02	V rot 90°, sp2

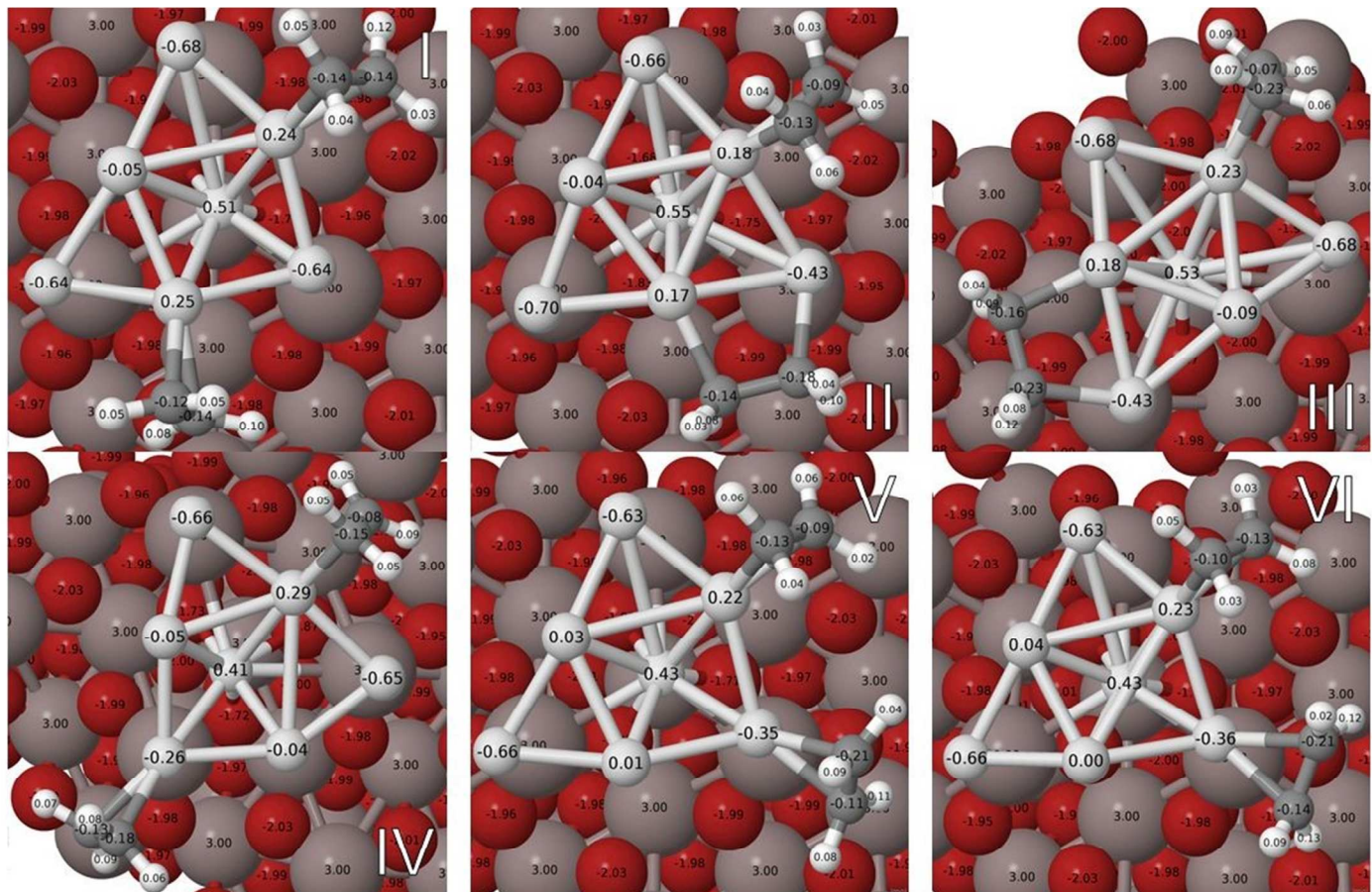


Figure S12. The lowest minima of 2 ethylene adsorbed on the Pt₇, Isomer I (the global minimum).

Table S7. Local minima configurations of a coverage of 3 ethylene on Pt₇,_{glob}

Configurations	P _{450 K}	P _{700 K}	ΔE	ΔQ _{Ethylene (e)}	Hybrid.
I	84.26%	69.22%	0.00	-0.30	2sp2, sp3
II	11.47%	19.21%	0.08	-0.08	3 sp2
III	4.02%	9.78%	0.12	-0.07	3 sp2
IV	0.24%	1.60%	0.23	0.07	3 sp2
V	>0.00%	0.12%	0.38	-0.04	3 sp2
VI	>0.00%	0.07%	0.41	-0.08	3 sp2

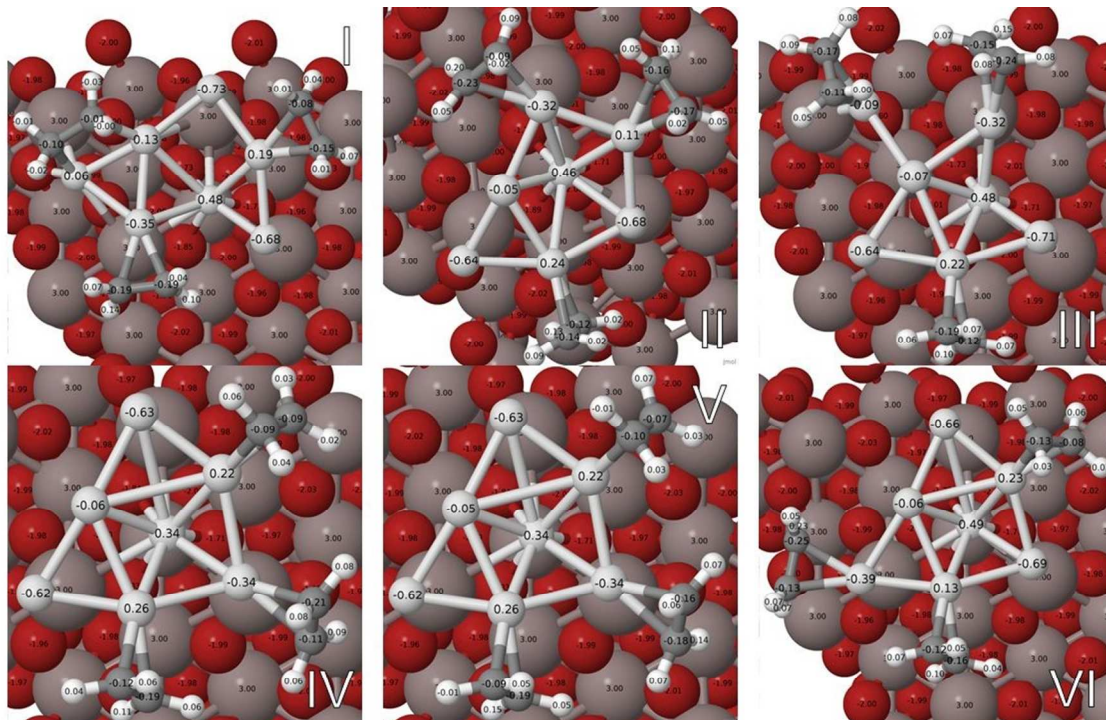


Figure S13. The lowest minima of 3 ethylene adsorbed on the Pt₇, isomer I (the global minimum).

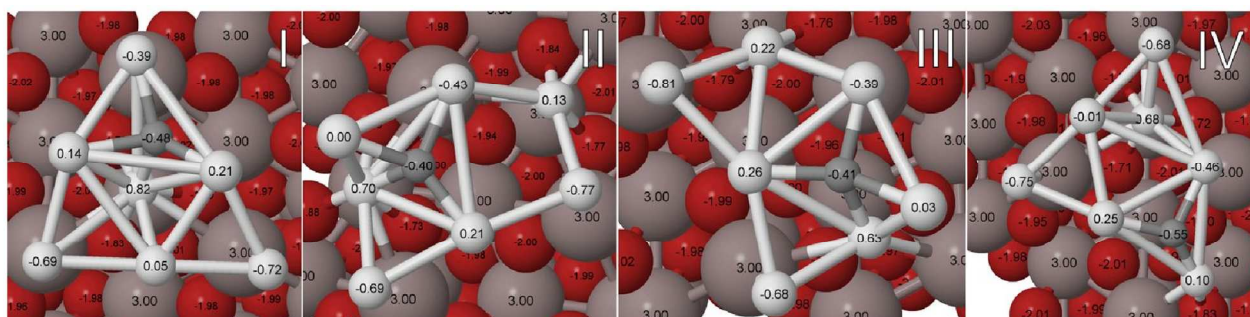


Figure S14. The C-sticking configurations of the lowest four isomers of Pt₇, with calculated Bader charges.

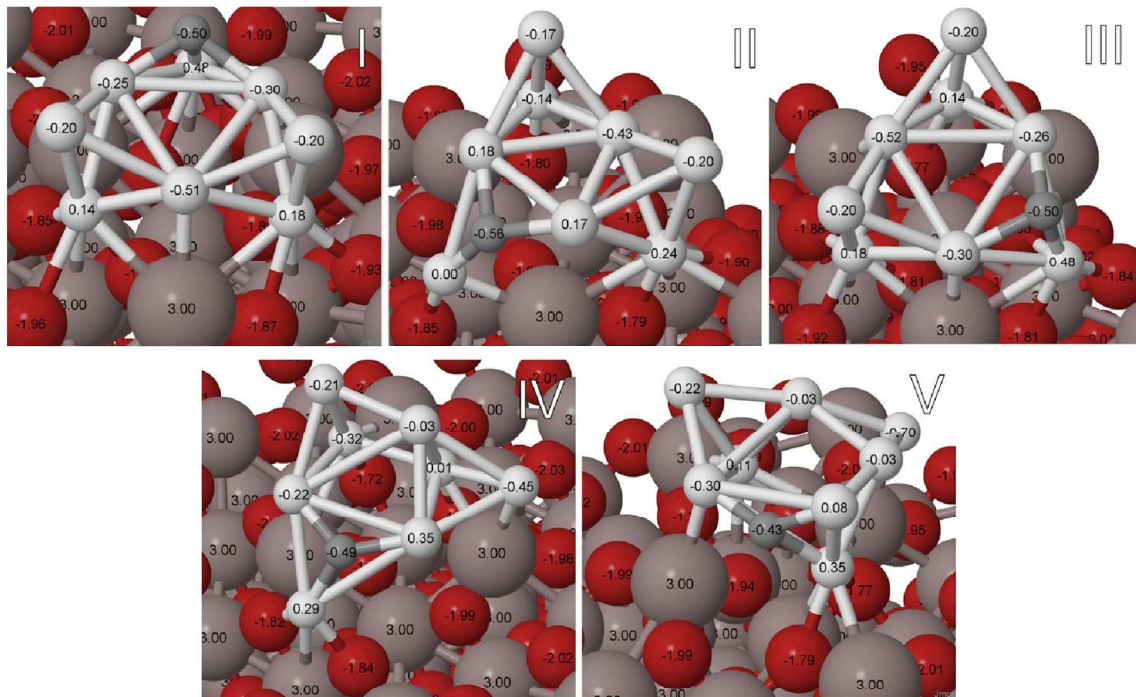


Figure S15. The C-sticking configurations of the lowest five isomers of Pt_8 , with calculated Bader charges.

References

1. Zhai, H.; Ha, M.; Alexandrova, A. N. *J. Chem. Theor. Comput.* **2015**, *11*, 2385-2393.
2. Tian, W. Q.; Ge, M.; Sahu, B.; Wang, D.; Yamada, T.; Mashiko, S. *J. Phys. Chem. A* **2004**, *108*, 3806-3812.